Heliyon 10 (2024) e28880

Contents lists available at ScienceDirect

Heliyon

journal homepage: www.cell.com/heliyon

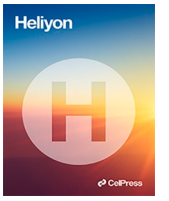

Research article

Osteogenic differentiation of human mesenchymal stem cells on electroactive substrates

M.N. Tamaño-Machiavello [a], E.O. Carvalho [b], D. Correia [c], L. Cordón [d,e], S. Lanceros-Méndez [b,f,g], A. Sempere [d,e,h], R. Sabater i Serra [a,i,*], J.L. Gómez Ribelles [a,i]

[a] Centre for Biomaterials and Tissue Engineering, CBIT, Universitat Politècnica de València, 46022 València, Spain
[b] Centre of Physics, Universidade do Minho, 4710-057, Braga, Portugal
[c] Centre of Chemistry, University of Minho, 4710-057, Braga, Portugal
[d] Hematology Research Group, Instituto de Investigación Sanitaria La Fe, València, Spain
[e] Centro de Investigación Biomédica en Red de Cáncer (CIBERONC), Instituto Carlos III, Madrid, Spain
[f] BCMaterials, Basque Center for Materials, Applications and Nanostructures, UPV/EHU Science Park, 48940, Leioa, Spain
[g] IKERBASQUE, Basque Foundation for Science, 48009, Bilbao, Spain
[h] Hematology Department, Hospital Universitario y Politécnico La Fe, València, Spain
[i] CIBER de Bioingeniería, Biomateriales y Nanomedicina, Instituto de Salud Carlos III, Spain

ARTICLE INFO

Keywords:
poly(vinylidene fluoride)
Electroactive cell substrates
Human bone marrow mesenchymal cells
Multipotency markers

ABSTRACT

This study investigates the effect of electroactivity and electrical charge distribution on the biological response of human bone marrow stem cells (hBMSCs) cultured in monolayer on flat poly(vinylidene fluoride), PVDF, substrates. Differences in cell behaviour, including proliferation, expression of multipotency markers CD90, CD105 and CD73, and expression of genes characteristic of different mesenchymal lineages, were observed both during expansion in basal medium before reaching confluence and in confluent cultures in osteogenic induction medium. The crystallisation of PVDF in the electrically neutral α-phase or in the electroactive phase β, both unpoled and poled, has been found to have an important influence on the biological response. In addition, the presence of a permanent positive or negative surface electrical charge distribution in phase β substrates has also shown a significant effect on cell behaviour.

1. Introduction

Mesenchymal stem cells (MSCs) are multipotent progenitor cells. They were first isolated from bone marrow by Friedenstein et al., who described them as adherent cells with fibroblastic morphology. They have the capacity of self-renewal and also the ability to differentiate to various cell types, including the chondrogenic, osteogenic, adipogenic and myogenic lineages [1,2]. MSCs can be obtained from bone marrow, adipose tissue, umbilical cord, and dental tissue [3,4]. Bone marrow mesenchymal stem cells (hBMSCs) are the most well-known and characterised source of adult stem cells. They have been used in bone regeneration research and are being validated in therapy clinical trials [4]. Adipose-derived mesenchymal stem cells (hASCs) are an alternative source of MSCs used in many studies [5]. *In vivo* studies have reported that MSCs derived from bone marrow induces more bone formation than MSCs from adipose tissue [6,7], which corroborate the suggestion that osteogenic progenitor predominantly populate bone marrow, whereas

* Corresponding author. Centre for Biomaterials and Tissue Engineering, CBIT, Universitat Politècnica de València, 46022, València, Spain.
E-mail address: rsabater@die.upv.es (R. Sabater i Serra).

https://doi.org/10.1016/j.heliyon.2024.e28880
Received 19 October 2023; Received in revised form 26 March 2024; Accepted 26 March 2024
Available online 29 March 2024

adipose tissue is mainly populated by adipogenic progenitors [8]. However, there is still controversy regarding the osteogenic capacity of adipose-derived MSCs compared to BMSCs [9].

CD105, CD90 and CD73 antigens are characteristic of the multipotency of hBMSCs; one of the conditions for their identification is that more than 95% of the hBMSCs population express these markers and that they lack hematopoietic antigens such as CD34, CD45, CD19, HLA-DR [10]. Decreased expression of one or more of these markers is associated with the commitment of hBMSCs to a particular lineage, and it is observed *in vitro* cultures early in the onset of differentiation [11–13].

When cultured on specific flat supports, in particular on tissue culture polystyrene (TCPS), MSCs can be expanded to high numbers while maintaining their multipotentiality, i.e. their capacity for osteogenic, chondrogenic and adipogenic differentiation [10]. This differentiation to each of the mentioned lineages can be induced by chemical means in specific configurations: osteogenic differentiation is induced with culture media containing dexamethasone, ascorbic acid, and in particular, growth factors of the morphogenetic protein family, such as Bone Morphogenetic Protein 2 (BMP2) [14]; chondrogenic differentiation is obtained in 3D configurations with high cell density and with culture media containing growth factors such as Transforming Growth Factor beta **(**TFG-β1, TFG-β3) and others; adipogenic differentiation is obtained by incubating the culture with dexamethasone, 3-isobutyl-1-methyl-xanthine (IBMX), insulin and indomethacin; in addition to these, triiodothyronine (T3), Asc-2-P and basic Fibroblast Growth Factor (bFGF-2) are also used [14].

However, it has been shown that specific physical characteristics of the substrate to which the cells adhere and proliferate are inducers of their loss of multipotentiality, committing the cells to a particular lineage. Among these factors, nano- or micro-topography has been highlighted. Thus, it has been shown that certain nanopatterning induces osteogenic differentiation [15,16]: on nanofiber supports, fibre order (random or aligned) determines adhesion, cell morphology and maintenance of phenotype or osteogenic differentiation [17,18]; substrate porosity is also determinant for the induction of differentiation [19], independently of chemical signalling. Substrate stiffness is also a determining factor in the fate of MSCs [20]. Further, physical stimulation can induce osteogenic or chondrogenic differentiation [21,22]. Surface electrical charge is among these physical factors, and it has been shown that a surface charge density affects the adhesion of MSCs to the substrate, spreading, and their proliferation and osteogenic differentiation [23–25]. To use mesenchymal stem cells (MSCs) for osteoregeneration therapies, it is necessary to develop efficient protocols for directing their differentiation into the osteogenic lineage *in vitro*. Besides, directing osteogenic differentiation of MSCs cells *in vitro* will provide models that are more amenable to molecular characterisation and genetic manipulation.

Poly(vinylidene fluoride), PVDF, is a semi-crystalline polymer, biocompatible, non-toxic and biostable polymer with great potential for tissue engineering due to its intrinsic piezoelectric properties [26]. Considering the piezoelectric properties of the bone tissue, PVDF substrates have been studied to prepare scaffolds which induce osteogenic differentiation of MSCs [27,28]. Abazari et at. prepared hybrid nanofibers based on PVDF/collagen/platelet-rich plasma nanofibers [29] and PVDF/PCL/basic fibroblast growth factor (bFGF) [30] to investigate their potential to stimulate osteogenic differentiation of induced pluripotent stem cells (iPSCs). Both systems demonstrated their osteoinductivity potential to be used as bone bio-implants for bone tissue engineering.

PVDF has the ability to crystallise in different orderings, showing at least 5 crystalline phases α, β, γ, δ and ε, being β phase the one showing the highest piezoelectric coefficient [31,32]. It has been shown that flat PVDF substrates in electroactive β-phase and polarised with positive or negative electrical surface charge adsorbed more fibronectin and exposed cell adhesion sequences more effectively than uncharged substrates, either in β-phase or α-phase. This fact affected the proliferation of MC3T3-E1 preosteoblasts [33]. The surface electric charge on electroactive PVDF supports significantly favoured the proliferation and osteogenic differentiation of hASCs [34].

The effect of PVDF substrate topography on cell response has been studied on non-electroactive α-phase PVDF supports on which microspheres, also of PVDF, were deposited by electro spraying. These microspheres, a few microns in diameter, crystallise in β-phase. It was seen how microtopography affected the morphology adopted by the cells on the support and the maintenance of their multipotency in expansion medium [35].

This study investigates the biological response of hBMSCs cultured on PVDF flat substrates with different crystallisation (α- and β-phase) and positive and negative charge surface density. We hypothesise that the piezoelectric properties and the electrical charge surface could drive hBMSCs from pluripotency to lineage commitment, focusing on osteogenesis. The maintenance of multipotency markers was analysed by flow cytometry, while the expression of characteristic genes osteogenic, chondrogenic and adipogenic differentiation was analysed by RT-qPCR. Alkaline phosphatase activity, as an osteogenic marker, was also assessed. Our objective was to investigate whether the different substrates induced spontaneous differentiation towards the osteogenic lineage (both with basal or osteogenic medium) or, on the contrary, the substrate properties compromised the cells towards other lineages, decreasing their capacity for osteogenic differentiation.

2. Materials and methods

2.1. Culture substrates

Poled and unpoled PVDF flat commercial substrates (films) crystallised in β phase with a thickness of 2.8 μm were supplied by Measurements Specialties, Inc. (Fairfield, NJ, USA). The poled β-PVDF films provided by that company were obtained using a static electrical potential (positive or negative) of several kV and used as received. Its degree of crystallinity is 55% and the fraction of β-phase crystals is above 95% [36,37]. Films of PVDF crystallised in α-phase, with 2.8 μm thickness, were also obtained from Measurements Specialties, Inc. The substrates were designed as ALPHA (PVDF crystallised in α-phase), BETA (unpoled PVDF crystallised in β phase), BETA (+) (positive poled PVDF crystallised in β phase), and BETA (−) (negative poled PVDF crystallised in β phase).

All the cell substrates were sterilised with ultraviolet (UV) light overnight, followed by three consecutive washing for 10 min with Dulbecco's Phosphate-Buffered Saline (DPBS) (Thermo Fisher, Waltham, MA, USA).

2.2. Fibronectin adsorption

Fibronectin (FN) from human plasma (Sigma-Aldrich, St. Louis, MO, USA) was adsorbed onto the PVDF samples. The films were immersed in a 20 μg/mL FN solution for 1 h under constant shaking. After protein adsorption, the samples were rinsed in saline solution to eliminate the non-adsorbed protein.

2.3. Obtention and characterisation of primary hBMSCs

Primary hBMSCs were obtained from bone marrow (BM) aspirates from patients with suspected, but finally, no alterations present, of hematological disease. Informed consent was obtained from the patients, following the established protocols of the Hospital Universitario y Politécnico La Fe (Valencia, Spain). hBMSCs from a young donor (<35 years old, male) were used in this study.

First, a pre-separation of the mononuclear cells was performed by density gradient (Ficoll-Hypaque system). Briefly, the BM samples were diluted in Dulbecco's Modified Eagle's Medium (DMEM) with ethylenediaminetetraacetic acid (EDTA) or heparin in a ratio 1:2 and the mixture was centrifuged at 1000×*g* for 30 min. The hBMSC-enriched cell population above the Ficoll layer was collected and washed thrice in DMEM by centrifugation at 400×*g* for 10 min. Finally, the cells were seeded (density: 1.8 x 10^5 cell/cm^2) and cultured at 37 °C and 5% CO2 with DMEM supplemented with 10% FBS, 100 U/mL penicillin-streptomycin (P/S, Invitrogen) and 2.5 mg/L amphotericin B (Sigma Aldrich). The culture medium was changed after 24–48 h, and non-adherent cells were removed. When the cells reached 85% confluence, they were trypsinised, centrifuged at 400×*g* for 5 min and, after discarding the supernatant, seeded again at a density of 3500–4000 cells/cm^2. After four passages, the cells were cryopreserved in liquid N_2.

The characterisation of hBMSCs was carried out by analysing the morphology of adhered cells to plastic, the specific surface antigen expression by flow cytometry, and their potential for multipotent differentiation [10]. It has been shown that hBMSC differentiated to osteoblasts, adipocytes and chondroblasts using *in vitro* tissue culture-differentiating conditions [38], as shown in the Supporting Information (Supplementary Materials and Methods).

2.4. Cell culture on the flat PVDF substrates (5 days)

Isolated hBMSCs (passage 5) were seeded onto the flat PVDF films (ALPHA, BETA, BETA (+), BETA (−)) and cultured with basal medium (DMEM containing 1 g/L glucose supplemented with 0.5% amphotericin B, 1% P/S, 10% FBS) at 37 °C, 5% CO_2. The culture medium was refreshed every two days. Cells seeded in tissue culture polystyrene supports (TCPS) were used as controls.

2.4.1. Phenotype assessment by flow cytometry

After 5 days of culture (PVDF substrates with diameter 11 mm, density of $1{\cdot}10^4$ cells/cm^2 p24-well plate, five biological triplicates), cells were lysed and collected for the analysis of the cellular immunophenotype. The cells were resuspended in 1 mL of medium, split into three aliquots differentially labelled and centrifugated at 300×*g* for 10 min. After removing the supernatant, cells were resuspended in 80 μL of DPBS, and 20 μL of FcR Blocking Reagent (Miltenyi Biotec) was added to block unspecific binding. Anti-human monoclonal antibodies conjugated with fluorescein isothiocyanate (FITC), phycoerythrin (PE), peridinin chlorophyll-cyanin protein (PerCP-Cy5.5), and alophycocianin (APC) were used: CD90-FITC[1], CD105-PE[1], HLA-DR-PerCP-Cy5.5[2], and CD73-APC[1] ([1]Miltenyi Biotec, [2]Becton Dickinson). The samples were processed using a FacsCanto-II™ flow cytometer, and 10000 events/sample were acquired. The marker expression percentages were obtained by FACSDiva 8.0.1 software (Becton Dickinson). Unstained hBMSCs were used as control. The analysis with the flow cytometer was performed in duplicate.

2.4.2. Cell viability

A MTS (3-(4,5-dimethylthiazol-2-yl)-5-(3-carboxymethoxyphenyl)-2-(4-sulfophenyl)-2H-tetrazolium) assay was carried out to quantify viable cells in proliferation after 3 and 5 days of cell culture (basal medium, cell density: 10^4 cells/cm^2) on previously sterilised flat PVDF supports (diameter: 11 mm) placed into p24-well plates (in triplicate). At every time point, the culture medium was replaced by DMEM without phenol red (Thermo Fisher) with 5:1 proportion of MTS (Promega) and left incubating for 3 h at 37 °C in the dark to allow MTS metabolisation. Then, 1 mL of supernatant was collected, and the absorbance was measured at 490 nm. A solution of MTS and DMEM without phenol red was used as reference (blank), and the supernatant (1 mL) of cells cultured in TCPS was considered the positive control. A calibration curve was performed to determine the number of viable cells. Data were expressed as triplicate samples' mean ± standard deviation (SD).

2.4.3. Cell morphology

Cell morphology was assessed by hematoxylin–eosin staining after 3 days of culture in p48-well plate (cell substrates diameter: 6 mm, 10^4 cells/cm^2, basal medium). The cells were fixed with a formaldehyde fixing solution to preserve the cell structure. Then, cells were stained with Mayer's hematoxylin (Sigma-Aldrich) for 15 min and washed with distilled water for 15 min. After that, the samples were submerged in Eosin Y (Sigma-Aldrich) for 2 min, washed with mQ water and mounted in a microscope slide with a mounting medium. After drying for 24 h, the samples were observed using a Leica DMD108 digital microscope. Each condition was studied with five biological replicates.

2.4.4. Gene expression analysis (RT-qPCR)

The expression of characteristic genes related to osteogenic differentiation (collagen type 1 (COL1A1), and Runx-related transcription factor 2 (RUNX2), adipogenic differentiation (lipoprotein lipase (LPL) and chondrogenic differentiation (SRY-related high-mobility-group box 9 (SOX9) was analysed by RT-qPCR after 5 days of culture (cell substrates diameter: 6 mm, p24-well plates, 10^4 cells/cm^2, basal medium). Total RNA was extracted by a Quick RNA Miniprep kit (ZYMO Research) and quantified by the NanoDropTM spectrophotometer (Thermo Scientific) at 260 nm. Then, it was reversed transcribed to cDNA (Maxima First Strand cDNA Synthesis Kit with Thermolabile dsDNase (ThermoFisher). The relative expression of the genes) was measured by RT-qPCR (ViiATM 7 Real-Time PCR System, Applied Biosystems). TaqMan assays (Universal Master Mix II from Applied Biosystems, Life Technologies) for COL1A1 (Hs00164004_m1), SOX9 (Hs01001343_g1), RUNX2 (Hs01047973_m1) and LPL (Hs00173425_m1) were used, with GAPDH (Hs03929097_g1) as the housekeeping gene. Each condition was studied with three biological replicates.

The q-PCR results were obtained from the relative quantification of gene expression, calculated by the comparative $2^{-\Delta\Delta Ct}$ method. The samples were normalised to the C_T value of the housekeeping gene (GAPDH): $\Delta C_T = C_T(sample) - C_T(\text{GAPDH})$. C_T control values were those obtained: $\Delta\Delta C_T = \Delta C_T(experiments) - \Delta C_T(control)$. Relative mRNA expression was obtained according to the following expression (Equation (1)):

$$Fold\ change = 2^{\Delta\Delta C_T} \tag{1}$$

2.5. Osteogenic differentiation on flat PVDF substrates

Isolated hBMSCs (passage 5) were seeded at a density of $1{\cdot}10^4$ cells/cm^2 onto the flat PVDF films (ALPHA, BETA, BETA (+), BETA (−)) with 11 mm of diameter and cultured with basal medium (p24-well plate) at 37 °C and 5% CO_2 for 5 days until they reached 100% confluence. Then, the osteogenic medium [DMEM containing 1 g/L glucose supplemented with 0.5% amphotericin B, 1% P/S, 10% FBS, 10 mM of β-Glycerophosphate disodium salt hydrate (Sigma Aldrich), 10 nM of dexamethasone-water soluble (Sigma Aldrich) and 50 μM of L-Ascorbic acid 2-phosphate sesquimagnesium salt hydrate (Sigma Aldrich)] was added, and cells were cultured for 28 days. In a parallel culture, hBMSCs were cultured in basal medium (without osteogenic supplements) on the same materials for 28 additional days after reaching 100% confluence. The culture medium was refreshed every 3 days. Cells seeded in TCPS were used as controls. Each condition was studied with three biological replicates.

2.5.1. Flow cytometry study

After 28 days of culture in osteogenic medium or basal medium after confluence, cells were lysed and collected. The surface markers CD105, CD90, CD73 and HLA-DR were analysed by flow cytometry using the protocol described in Section 2.4.1.

2.5.2. Analysis of alkaline phosphatase (ALP) activity

After 7 and 14 days of culture (both in osteogenic medium and basal medium after confluence), the cells were lysed and collected. The level of ALP present on each sample was determined in cell lysates by a SensoLyte® pNPP Alkaline Phosphatase Assay Kit (ANASPEC), and the total protein of the lysate was determined using a Micro BCA™ Protein Assay Kit (Thermo Scientific). The ALP activity was obtained as the ratio between ALP and total protein. Each condition was studied with three biological replicates.

2.5.3. Gene expression analysis (RT-qPCR)

The expression of characteristic genes related to osteogenic differentiation COL1A1 (Hs00164004_m1), RUNX2 (Hs01047973_m1) and integrin-binding sialoprotein (IBSP) (Hs00173720_m1) was analysed after 28 days of cell culture (both in osteogenic medium and basal medium after confluence) by RT-qPCR using the protocol described in section 2.4.4, with GAPDH (Hs03929097_g1) as the housekeeping gene.

2.6. Statistical analysis

The results were expressed as the mean ± SD. All quantitative data were analysed using GraphPad Prism (v6.00, La Jolla, CA, USA). The results were analysed statistically using a one-way ANOVA test and Tukey's multiple comparisons test. Differences were considered significant when $p < 0.05$.

3. Results and discussion

3.1. Characterisation of primary hBMSCs

The hBMSCs cultured in TCPS wells adhered to the plastic, showing a homogeneous fibroblastoid morphology (Supplementary Fig. S1). Regarding the immunophenotypic markers, the experimental flow cytometry results (Supplementary Fig. S2) revealed that the cells expressed CD105, CD90 and CD73 antigens, which are characteristic of the hBMSCs. One of the conditions for their identification is that more than 95% of the hBMSCs population express these markers and that lack hematopoietic antigens such as CD34, CD45, CD19 or HLA-DR. It can be observed in Supplementary Fig. S2 that the expression of HLA-DR is negative except for a small percentage of hMSCs (1.9 % HLA-DR+), which could be explained as an effect of cell activation. The capacity of adipogenic, osteogenic and chondrogenic differentiation was demonstrated with oil red O, alizarin red S and safranin O staining, respectively (Supplementary

Fig. S3). The oil red O staining showed the formation of lipid vacuoles inside the labelled cells when cultured in adipogenic medium. On the other hand, osteogenic medium caused a change in the growth pattern and distribution of the cultured cells, which resulted in the formation of cell nodules that showed signs of mineralisation after staining with alizarin red. Finally, the three-dimensional pellet culture of the cell populations cultured in chondrogenic medium caused a change in cell morphology from a fusiform to a rounded shape. Safranin O staining revealed the presence of proteoglycans.

3.2. Non-confluent cell growth in basal medium

The hBMSCs adhered and proliferated, reaching confluence after 6 days of culture in basal medium. Therefore, in the first stage, viability, proliferation, multipotency marker expression and gene expression at day 5 (before reaching confluence), a time-point that represents a behavioural change in the cellular response, was characterised. Hematoxylin and eosin staining (Fig. 1A) revealed that the cells adhered to all PVDF substrates. hBMSCs adhered to unpoled BETA substrates showed a round morphology, while on BETA (+) substrates, cells showed more homogeneity in shape and size. More elongated shape was observed in hBMSCs cultures on ALPHA and BETA (−) substrates, although BETA (−) substrates showed higher cell spreading with elongated filopodia. The viability measured in the MTS assay showed that the numbers of viable cells in the BETA (+) samples were significantly lower than those found in the other PVDF supports. No significant differences were found among ALPHA, BETA and BETA (−) substrates and TCPS control after 5 days of culture (Fig. 1B).

Flow cytometry assay after 5 days of culture (Fig. 2) revealed that the cells cultured on the PVDF sample crystallised in the non-polar α-phase, PVDF (ALPHA), as well as on the TCPS control, maintained the expression of the three markers CD105, CD90 and CD73, unaltered with respect to those of the cells initially seeded on the supports (Supplementary Fig. 2S). Nevertheless, the behaviour of the cells seeded onto the supports in polarised or non-polarised polar β-phase samples changed significantly. When analysing cell behaviour, it is interesting to note the differences among the different supports of electroactive β-phase crystallised PVDF. While α-phase crystallisation leads to an ordering of the polymer chains that make them electrically neutral, β-phase crystallisation in all-trans conformation causes each chain to have a net permanent dipole moment [32,39]. The surface remains, on average, neutral because the crystals appearing in the vicinity of the surface are randomly oriented, and the sum of their charges would be zero if measured in macroscopic dimensions [40]. However, locally, in dimensions comparable to crystal sizes, which may be on the order of a micron or a few microns, there is a net charge that depends on the orientation of that specific crystal, and the cells can sense those local electric fields. That is, the difference in terms of the physical characteristics of ALPHA and BETA substrates lies in the presence of those electric charges at the local level in the β-phase. It has been reported that there are also differences in topography (the shape of the crystalline spherulites, the crystal sizes and the surface roughness are different in one phase and the other) [41,42]. In poled samples, the crystalline regions are oriented in such a way that the permanent dipolar moments are aligned with each other. Thus, a positive or negative charge distribution is generated depending on the orientation of the electric field [40].

It is interesting to note that, in both unpoled BETA and poled BETA (+) supports, the distribution bells of the CD105 and CD90 markers (Fig. 2A) widen with respect to those before cell seeding (Supplementary Fig. S2), which can be interpreted in the sense of a greater heterogeneity in the cell population. Even in the case of BETA (+), the distribution shows a clear heterogeneous pattern, indicating the separation of two populations with different expression of the multipotency markers. Moreover, the distributions are

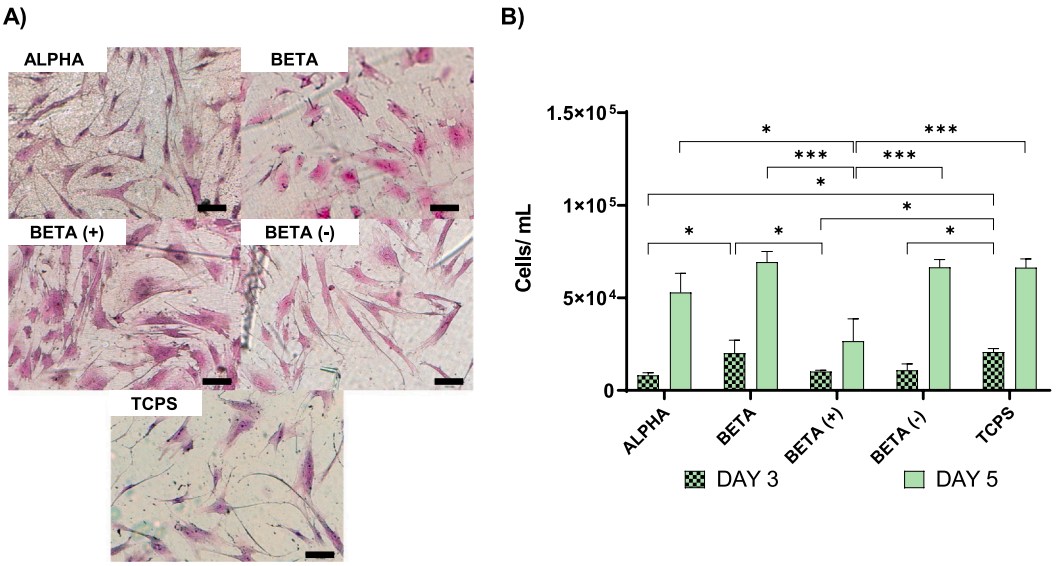

Fig. 1. A) Hematoxylin–eosin staining after 3 days of culture on PVDF films (ALPHA, BETA, BETA (+) and BETA (−)). Scale bar: 100 μm. B) hBMSCs proliferation (cells/mL) after 3 and 5 days of culture with basal medium on PVDF films: ALPHA, BETA, BETA (+) and BETA (−). Cells cultured on TCPS were used as control. Results are expressed as mean ± SD (n = 3). (*) $p < 0.05$, (**) $p < 0.01$, (***) $p < 0.001$).

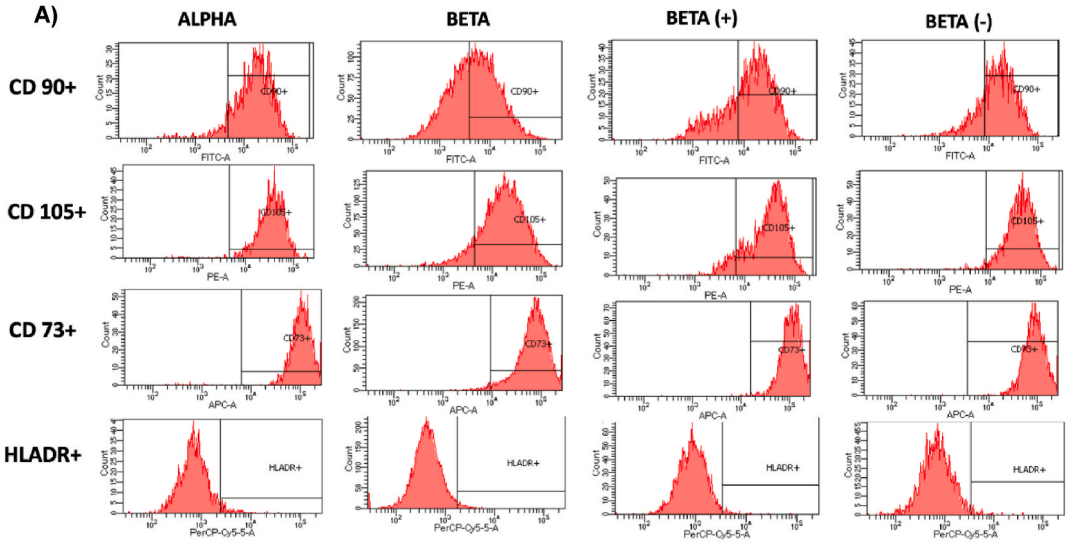

B)

SAMPLES BM (5 days)	CD 90+	CD105+	CD73+	HLADR+
TCPS	94.1 ± 1.9	97.5 ± 0.1	99.1 ± 0.1	3.4 ± 2.7
ALPHA	81.3 ± 14	98 ± 0.0	98.8 ± 0.3	4.3 ± 0.8
BETA	51.6 ± 6.9	90.2 ± 3.2	93.8 ± 2.8	4.6 ± 1.7
BETA (+)	66.7 ± 3.8	85.5 ± 5.0	97.1 ± 2.3	3.3 ± 0.6
BETA (-)	73.0 ± 4.5	95.2 ± 2.5	97.6 ± 2.2	2.7 ± 0.4

Fig. 2. Immunophenotypic analysis by flow cytometry after 5 days of culture on TCPS and PVDF films ALPHA, BETA, BETA (+) and BETA with basal medium. A) Histograms of hBMSCs showing the expression of surface proteins CD90, CD105, CD73 and HLA-DR surface markers. B) Percentage of expression of surface proteins (−). Number of events acquired: 10^4.

shifted to the left. The fraction of positive cells with respect to each marker are included in Fig. 2B. It is evidenced that while in ALPHA and the TCPS control support more than 90% of the cells maintain positive labelling to CD105, CD90 and CD73, the percentage of positive CD90 cells drops until below 55% and 70% in BETA and BETA (+), respectively. The expression of positive CD105 cells shows a minor decrease, until 90 and 85% in BETA and BETA (+) substrates, respectively. The case of the poled BETA (−) substrate is somewhat intermediate; while the percentage of CD105+ and $CD73^+$ is above 95%, that of $CD90^+$ has dropped to 73%, while the distribution bells are narrower than in BETA and BETA (+) substrates, indicating a more homogeneous cell population.

It has been reported [12] that in the initial stages of differentiation of cord blood-derived MSCs in osteogenic or adipogenic medium, there is a marked decrease in the expression of CD105 and CD90 markers, while that of CD73 remains above 95%. However, it was also found that the drop in the CD90 marker occurred only in the adipogenic differentiation [13]. Regarding chondrogenic differentiation, a drop in the three mentioned markers has been observed [43]. The decrease in CD105 and CD90 was also found after the first day of inducing chondrogenic differentiation [44].

The expression of four genes characteristic of osteogenic (COL1A1, RUNX2) [45,46], chondrogenic (SOX9) and adipogenic (LPL) differentiation was evaluated using RT-qPCR. RUNX2 is an early marker of osteogenic differentiation [45]. During osteogenic development, COL1A1 gene expression was observed 2 days after induction of osteogenic differentiation [47,48]. Finally, SOX9 is a transcription factor that controls chondrocyte-specific gene expression, which expression was detected early during chondrogenic differentiation [49]. Expression of LPL gene was observed at culture times of one week during adipogenic differentiation [50].

Cells expanded in TCPS for 5 days in basal medium, shown in Fig. 3, only express significant differences with respect to the hBMSCs expression before cell seeding (DAY 0) in terms of the COL1A1 gene marker, as expected (Fig. 3A). The α-phase PVDF support (ALPHA substrate) induced overexpression of RUNX2 with respect to the control, with differences that were also significant with respect to the expression at DAY 0 (Fig. 3B). The expression of SOX9 did not differ from that of the control (TCPS) but was slightly higher than at DAY 0 (Fig. 3C), while the mean value of LPL was higher than at DAY 0, despite the higher uncertainty of this result (Fig. 3D). In contrast, the electroactive β-phase clearly supports the induction of a lower expression of the four markers, except for SOX9 and COL1A1 expression in BETA (+) substrates, which was significantly higher than for the cells cultured on BETA and BETA (−) substrates, but with no significant difference with the TCPS (control). The mean value of RUNX2 expression was also higher in BETA (+) than in the other PVDF substrates in β phase, but the differences were not statistically significant. The lower proliferation found in BETA (+) substrates could also be related to the cells' higher commitment to the chondrogenic lineage.

3.3. Confluent cell cultures in basal and osteogenic medium

When culture was continued in basal medium for 28 additional days after confluence, hBMSCs spontaneously differentiated,

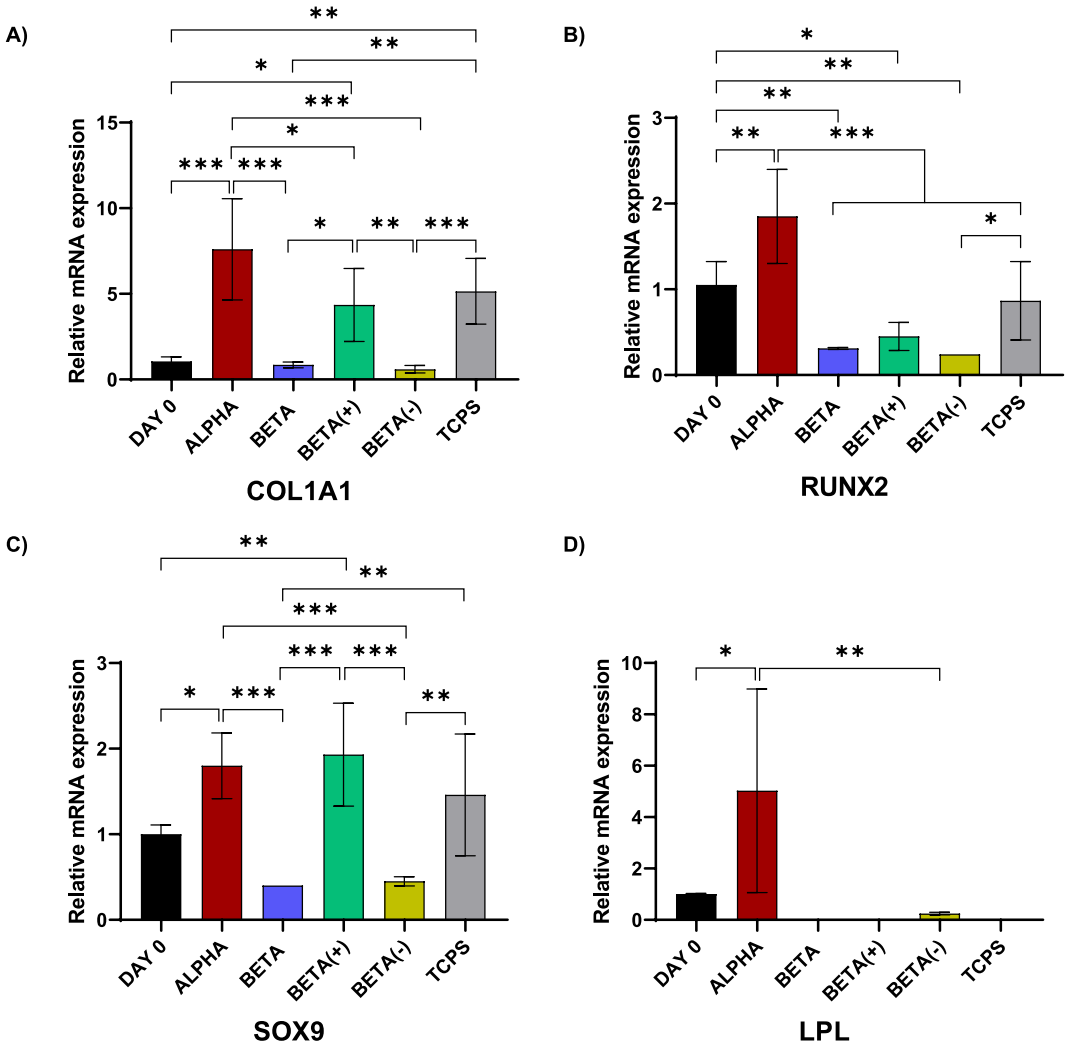

Fig. 3. Gene expression analysis (RT-qPCR) of COL1A1, LPL, SOX9 and RUNX2 after 5 days of culture on PVDF films (ALPHA, BETA, BETA (+) and BETA (−)) with basal medium. DAY 0: Gene expression of hBMSCs before seeding. Data presented as average ± SD (n = 3). (*) $p < 0.05$, (**) $p < 0.01$, (***) $p < 0.001$).

resulting in widening and displacement of the distribution bells of multipotency markers in flow cytometry (Fig. 4A). The quantification of this shift is shown in Fig. 4B. Compared to the expression of markers before cell seeding (Supplementary Fig. 2S), the expression of $CD90^+$ and CD105+ drops considerably in BETA and BETA (+) supports; the expression of $CD73^+$ also decreased, although more moderately. In the case of ALPHA and BETA (−) supports and in TCPS control, $CD90^+$ and CD105+ markers clearly also diminished, although to a lesser extent. These changes have been identified as indicative of MSCs differentiation into their different lineages [13,43,44].

ALP activity is considered an initial marker of osteogenic differentiation of MSCs [51]. In this study, the absence of alkaline phosphatase expression after 7 and 14 days of culture with basal medium indicates that osteogenic differentiation was residual (Fig. 5). The most significant indication of the role of the substrate in osteogenic differentiation was the expression of ALP in hBMSCs cultured with osteogenic medium after confluence. Although 7 days after introducing the osteogenic culture medium, there were no significant differences among the different PVDF supports (Fig. 5A), as the culture progressed (14 days), the expression of ALP in BETA (−) substrates was significantly higher than the rest of the PVDF supports, albeit it still fell below the expression in TCPS (Fig. 5B). These results are in line with those obtained by Pärssinen et a [42]. with hASCs cultured with basal or osteogenic medium on flat substrates prepared with α-PVDF, unpoled β-PVDF and poled β-PVDF. After 15 days of culture, ALP activity was very low when hASCs were cultured in basal medium. However, hACS cultured with osteogenic medium showed differences between substrates, with greater ALP activity on poled rather than unpoled PVDF substrates, although no significant differences were found between positive and negative poled β-PVDF. It is well known that the response of each cell lineage to electrical charge stimulation is unique [52]. However, the influence of different charge types on biomaterials on osteogenesis and their interdependent mechanisms have not been clearly defined yet. The higher ALP activity shown in this study by hBMSCs cultured on negatively charged β-PVDF substrates (BETA (−)) suggests that

A)

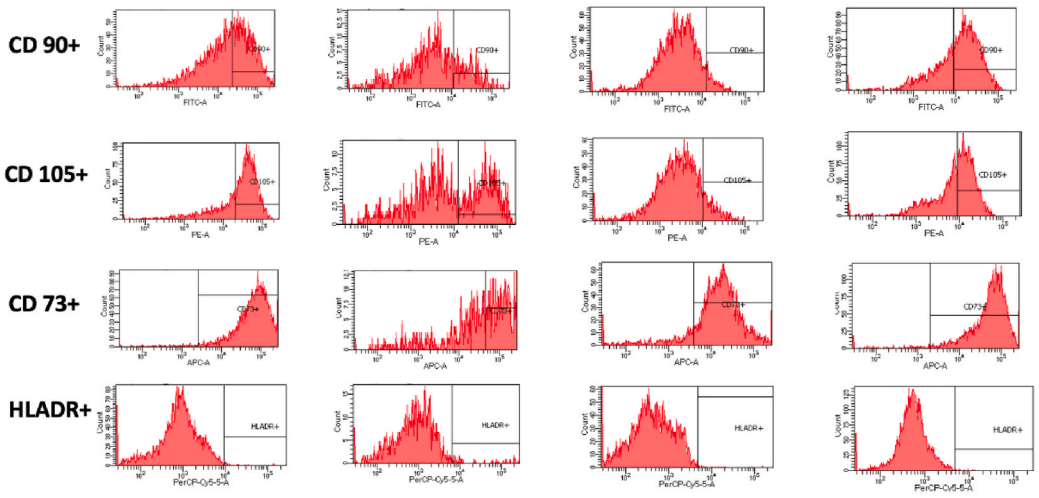

B)

SAMPLES BM (28 days)	CD 90+	CD105+	CD73+	HLADR+
TCPS	74.3 ± 0.0	72.3 ± 4.2	97.4 ± 2.1	1.1± 0.1
ALPHA	43.0 ± 3.5	66.4 ± 1.7	94.2 ± 2.5	1.45 ± 0.2
BETA	27.0 ± 2.8	45.5 ± 6.4	56.0 ± 4.2	2.9 ± 1.2
BETA (+)	7.5 ± 0.6	10.0 ± 2.5	56.0 ± 4.2	2.85 ± 1.2
BETA (-)	66.3 ± 5.2	48.8 ± 5.4	94.5 ± 0.7	1.3 ± 0.3

C)

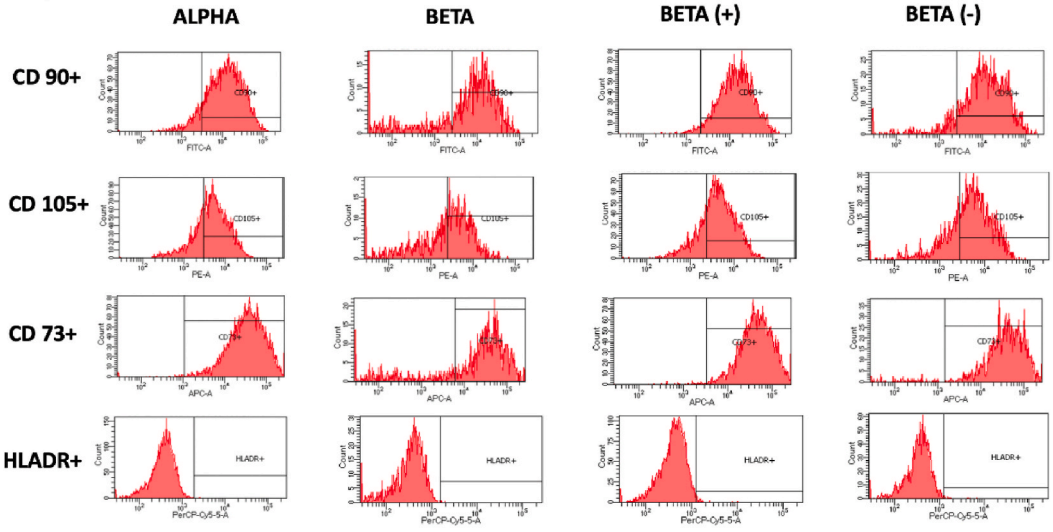

D)

SAMPLES OM (28 days)	CD 90+	CD105+	CD73+	HLADR+
TCPS	74.3 ± 5.7	47.8 ± 4.5	97.1 ± 2.6	1.3 ± 0.4
ALPHA	89.0 ± 1.7	65.9 ± 4.0	96.7 ± 1.8	1.1 ± 0.7
BETA	76.9 ± 1.6	53.2 ± 4.5	77.9 ± 0.1	0.85 ± 0.9
BETA (+)	93.5 ± 2.1	69.0 ± 5.6	97.1 ± 1.2	1.1 ± 0.4
BETA (-)	88.5 ± 3.5	64.6 ± 7.6	95.1 ± 0.1	1.2 ± 0.1

(caption on next page)

Fig. 4. Immunophenotypic analysis by flow cytometry. Immunophenotypic analysis by flow cytometry. (A) Histograms of hBMSCs showing the expression for CD90, CD105, CD73 and HLA-DR surface markers after 28 days of culture (after 100% confluence) on PVDF films (ALPHA, BETA, BETA (−), BETA (+) with basal medium and percentage of expression of stained hBMSCs surface markers (B). (C) Histograms of hBMSCs showing the expression for CD90, CD105, CD73 and HLA-DR surface markers after 28 days of culture on PVDF films (ALPHA, BETA, BETA (+), BETA (−)) with osteogenic medium and percentage of expression of stained hBMSCs surface markers (D). Number of events acquired (B and D): 10^4.

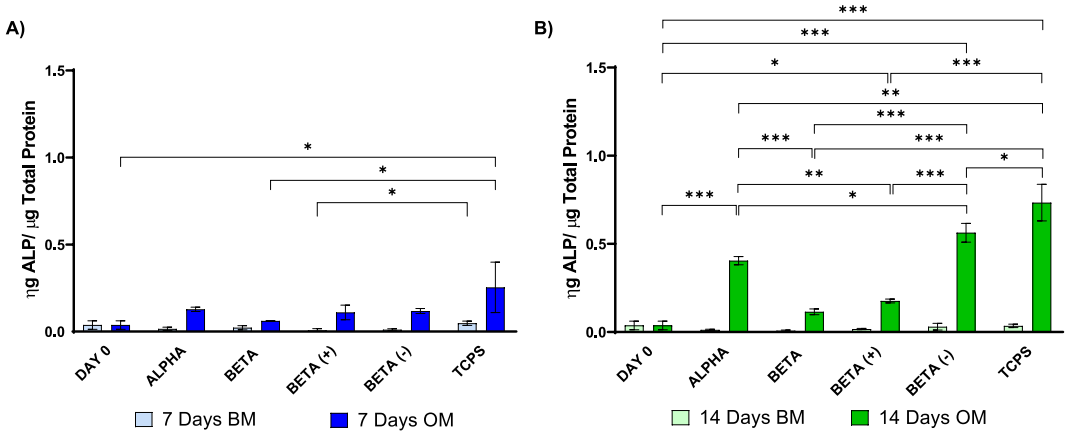

Fig. 5. Alkaline phosphatase (ALP) activity of hBMSCS at 7 days (A) and 14 days (B) of culture (after confluence) on PVDF films (ALPHA, BETA, BETA (+) and BETA (−)) with basal medium (BM) and osteogenic medium (OM). DAY 0: ALP activity of hBMSCs before seeding. Data presented as average ± SD (n = 3). (*) $p < 0.05$, (**) $p < 0.01$, (***) $p < 0.001$).

MSCs from bone marrow have a greater predisposition to osteogenic differentiation on this type of substrates (when cultured with osteogenic medium) than mesenchymal cells from adipose tissue.

In osteogenic medium, after 28 days of culture, the differences in cellular response in the different substrates became smaller (Fig. 4C). As expected, the expression of the multipotency antigens CD90 and CD105 (Fig. 4D) fell in all substrates with respect to the expression before cell seeding (Supplementary Fig. S2), although with differences depending on the crystalline phase and the polarity of the substrate. CD73 expression is maintained in all the substrates, except in the unpoled BETA, which shows a significant drop in CD73. Gene expression (measured by RT-qPCR) of COL1A1, RUNX2, and IBSP, osteogenic specific markers, are shown in Fig. 6. ALPHA and poled BETA (−) supports showed higher expression of COL1A1 compared to unpoled BETA and poled BETA (+) substrates (Fig. 6A). However, there were no significant differences in the expression of RUNX2 among the different substrates, although there were with respect to DAY 0 (Fig. 6B). The expression of the bone sialoprotein gene IBSP (Fig. 6C) was also measured, as it mediates cell attachment to hydroxyapatite in bone tissue and is an early mineralisation marker in osteogenic differentiation [53,54]. There were no significant differences in IBSP expression between the PVDF substrates, with values still below its expression in the TCPS control.

How the cell adheres to the substrate is crucial for its subsequent proliferation and differentiation. A detailed study of spreading and focal adhesions of hASCs showed that a negatively charged surface density on the substrate increases cell adhesion (higher adhesion area and number of adhesions per cell) [34]. Zhou et al. 2016 also found this increased adhesion in negatively poled PVDF coatings on titanium surfaces prepared via the tape-casting method [55]. They explained this fact by the increased adhesion of fibronectin to the substrate. The positive charges of the adsorbed FN layer would overcompensate the negative surface charges, exhibiting a cationic surface character that would electrostatically attract the cell membranes. The effect is the same as that which allows the production of

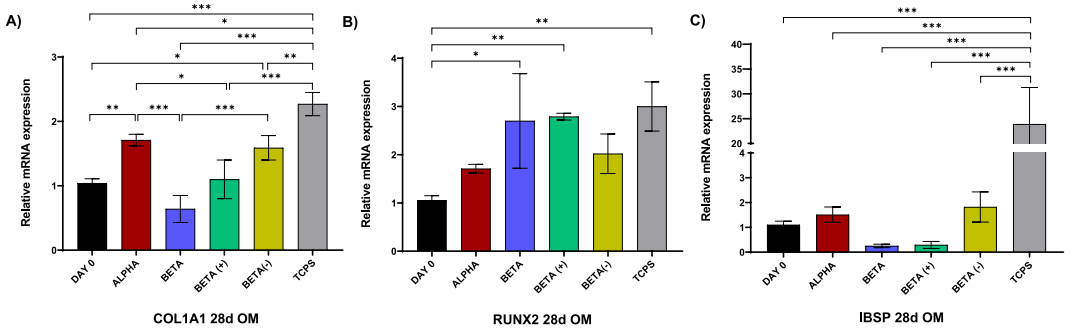

Fig. 6. Gene expression analysis (RT-qPCR) after 28 days of culture on PVDF films (ALPHA, BETA, BETA (+) and BETA (−)) with osteogenic medium. A) COL1A1, B) RUNX2 and C) IBSP. Data presented as average ± SD (n = 3). (*) $p < 0.05$, (**) $p < 0.01$, (***) $p < 0.001$).

polyelectrolyte multilayers by the layer-by-layer method. Ribeiro et al. [33] found that the amount of adhesion sequences exposed by the adsorbed FN layer on the substrate surface was higher on polarised electroactive PVDF than on non-polarised or crystallised in phase β, however, no statistically significant differences were found between the positively or negatively charged surface. It has been reported that cell shape plays an important role in lineage commitment. hMSCs allowed to adhere, latten and spread underwent osteogenesis, while those with a round morphology differentiated into adipocytes [56,57]. Our results suggest that BETA (−) substrates, and, to a lesser extent, ALPHA substrates, in which adhered hBMSCs showed an elongated morphology, could induce an early commitment towards osteogenic differentiation. In addition, we found that positive charge density significantly slows down cell proliferation, which agrees with previous studies [55,58]. Nevertheless, proliferation in the unpoled β surface was the same order as in BETA (−) substrates.

Taken as a whole, it appears that the presence of a net positive electric charge density on the substrate induces a loss of multipotency of the hBMSCs in basal medium, decreasing at the same time their proliferative capacity and compromising their subsequent differentiation to bone lineage cells when cultured in osteogenic differentiation medium. These effects can also be transferred to the crystallised support in β-phase but not polarised, as negative and positive charges will appear on the surface at a local level. On the contrary, negative charge density favours osteogenic differentiation, as indicated by the higher expression of ALP. At this point, the present results agree with those reported by Zhou et al. on different negatively charged polarised PVDF films on Ti surfaces [55]. The results are also consistent with those reported by Geng et al. [59], where they used a simplified model for a single-factor study based on graphene quantum dots (GQD) to analyse the effect of surface charge on osteogenic differentiation. Their study demonstrated that negative GQD significantly enhanced osteogenic differentiation of hBMSCs.

As stated previously, PVDF is biocompatible. However, it is a non-biodegradable polymer, which can lead to long-term accumulation in the body and cause adverse effects, such as inflammation and immune responses [60], limiting its use *in vivo* as a cell delivery vehicle. To overcome this disadvantage, we plan to use the PVDF cell substrates to condition the mesenchymal cells *in vitro,* inducing their commitment toward osteogenic differentiation and subsequently implant them in the bone defect using a biodegradable biomaterial, such as polylactic acid, polycaprolactone or hydrogels, as a vehicle to *in vivo* delivery of the primed cells.

Finally, the limitations of the present study should be highlighted. The study was conducted in a two-dimensional environment (flat substrates), far from the three-dimensional biological environment of *in vivo* systems. In addition, it should be taken into account that the study has been carried out based on the intrinsic piezoelectric and surface charge properties of the biomaterials used as cell substrates, without any type of external stimulation.

Future work will be focused on analysing cellular behaviour in three-dimensional environments, such as micro/nanofibers based on the same materials. Furthermore, incorporating electro-mechanical stimulation would allow for obtaining greater information about the behaviour of mesenchymal cells and their influence on adhesion, proliferation and the induction of osteogenic differentiation.

4. Conclusions

Substantial differences have been found in the biological response of human bone marrow mesenchymal stem cells, hBMSCs, cultured on crystallised α-phase. ALPHA, or in the electroactive β-phase PVDF substrates, BETA. Furthermore, significant differences have also been found between electroactive substrates non-polarised, BETA, or polarised with positive BETA (+) or negative, BETA (−) charge distribution. In basal medium, during the first days of expansion before reaching confluence, the α-phase substrates, like the TCPS control, maintain the expression of the multipotency markers. However, in the β-phase substrates there is a marked loss of the CD105 marker and in the non-polarised or positively charged substrates (BETA and BETA (+) also in CD90. In addition, the proliferation capacity of the hBMSCs on BETA (+) substrates is inferior to the rest of the substrates. The β-phase substrates, however, show a lower expression of genes characteristic of early differentiation. When cultured in osteogenic medium, CD90 and CD105 markers drop, as expected, in all substrates, while CD73 expression is maintained. In the negatively charged β-substrate BETA (−), ALP expression increases. This finding can correlate with a superior degree of osteogenic induction when contrasted with unpoled BETA and positively charged substrates BETA (+). These results suggest that osteogenic differentiation of hBMSCs is supported by negatively charged, electroactive polarised substrates. Conversely, non-polarised or positively polarised substrates appear to induce an early commitment of hBMSCs that renders osteogenic induction by chemical means ineffective. However, some challenges still need to be addressed to fully evaluate the potential of poled BETA (−) substrates to induce osteogenesis of hBMSCs. One of the main challenges is to investigate the effect of electro-mechanical stimulation, as well as optimize the parameters (frequency and amplitude) to direct osteogenic differentiation. Another challenge is developing and assessing three-dimensional scaffolds based on these materials. Despite these challenges, the use of cell substrates with a specific distribution of surface electrical charge able to induce osteogenic lineage commitment of MSCs, such as those investigated in this study, holds great promise for developing new therapies for bone-related diseases.

Data availability

Data will be made available on request.

CRediT authorship contribution statement

M.N. Tamaño-Machiavello: Writing – original draft, Visualization, Investigation, Formal analysis. **E.O. Carvalho:** Formal analysis. **D. Correia:** Formal analysis. **L. Cordón:** Writing – review & editing, Formal analysis. **S. Lanceros-Méndez:** Writing – review

& editing, Funding acquisition, Conceptualization. **A. Sempere:** Writing – review & editing, Conceptualization. **R. Sabater i Serra:** Writing – review & editing, Visualization, Supervision, Conceptualization. **J.L. Gómez Ribelles:** Writing – review & editing, Supervision, Funding acquisition, Conceptualization.

Declaration of competing interest

The authors declare that they have no known competing financial interests or personal relationships that could have appeared to influence the work reported in this paper.

Acknowledgements

This work has been supported by PID2022-138572OB-C41 and C42 projects funded by MCIN/AEI/10.13039/501100011033/FEDER, Spain/EU. The research was also supported by CIBER – Consorcio Centro de Investigación Biomédica en Red - CB06/01/1026, Instituto de Salud Carlos III (Ministerio de Ciencia e Innovación, Spain), and by the Portuguese Foundation for Science and Technology (FCT) under strategic funding UID/FIS/04650/2021, grant SFRH/BD/145455/2019 (EOC) and Investigator FCT Contract 2020.02915.CEECIND (D.M.C.). Support from the Basque Government Industry Department under the ELKARTEK program is also acknowledged.

Appendix A. Supplementary data

Supplementary data to this article can be found online at https://doi.org/10.1016/j.heliyon.2024.e28880.

References

[1] A. Friedenstein, R. Chailakhyan, N. Latsinik, A. Panasyuk, I. Keiliss-Borok, Stromal cells responsible for transferring the microenvironment of the hemopoietic tissues, Transplantation 17 (1974) 331–340.
[2] E.M. Horwitz, K. le Blanc, M. Dominici, I. Mueller, I. Slaper-Cortenbach, F.C. Marini, R.J. Deans, D.S. Krause, A. Keating, Clarification of the nomenclature for MSC: the international society for cellular therapy position statement, Cytotherapy 7 (2005) 393–395, https://doi.org/10.1080/14653240500319234.
[3] R. Hass, C. Kasper, S. Böhm, R. Jacobs, Different populations and sources of human mesenchymal stem cells (MSC): a comparison of adult and neonatal tissue-derived MSC, Cell Commun. Signal. 9 (2011), https://doi.org/10.1186/1478-811X-9-12.
[4] F. Shang, Y. Yu, S. Liu, L. Ming, Y. Zhang, Z. Zhou, J. Zhao, Y. Jin, Advancing application of mesenchymal stem cell-based bone tissue regeneration, Bioact. Mater. 6 (2021) 666–683, https://doi.org/10.1016/j.bioactmat.2020.08.014.
[5] G. Storti, M.G. Scioli, B.S. Kim, A. Orlandi, V. Cervelli, F. De Francesco, Adipose-derived stem cells in bone tissue engineering: useful tools with new applications, Stem Cell. Int. 2019 (2019), https://doi.org/10.1155/2019/3673857.
[6] G.P. Freitas, H.B. Lopes, A.L.G. Almeida, R.P.F. Abuna, R. Gimenes, L.E.B. Souza, D.T. Covas, M.M. Beloti, A.L. Rosa, Potential of osteoblastic cells derived from bone marrow and adipose tissue associated with a polymer/ceramic composite to repair bone tissue, Calcif. Tissue Int. 101 (2017) 312–320, https://doi.org/10.1007/s00223-017-0282-3.
[7] W. Zhang, X. Zhang, S. Wang, L. xu, M. Zhang, G. Wang, Y. Jin, X. Zhang, X. Jiang, Comparison of the use of adipose tissue–derived and bone marrow–derived stem cells for rapid bone regeneration, J. Dent. Res. 92 (2013) 1136–1141, https://doi.org/10.1177/0022034513507581.
[8] T.M. Liu, M. Martina, D.W. Hutmacher, J.H.P. Hui, E.H. Lee, B. Lim, Identification of common pathways mediating differentiation of bone marrow- and adipose tissue-derived human mesenchymal stem cells into three mesenchymal lineages, Stem Cell. 25 (2007) 750–760, https://doi.org/10.1634/stemcells.2006-0394.
[9] H.-T. Liao, Osteogenic potential: comparison between bone marrow and adipose-derived mesenchymal stem cells, World J. Stem Cell. 6 (2014) 288, https://doi.org/10.4252/wjsc.v6.i3.288.
[10] M. Dominici, K. le Blanc, I. Mueller, I. Slaper-Cortenbach, F.C. Marini, D.S. Krause, R.J. Deans, A. Keating, D.J. Prockop, E.M. Horwitz, Minimal criteria for defining multipotent mesenchymal stromal cells. The International Society for Cellular Therapy position statement, Cytotherapy 8 (2006) 315–317, https://doi.org/10.1080/14653240600855905.
[11] J.-W. Yang, N. de Isla, C. Huselstein, M.-N. Sarda-Kolopp, N. Li, Y.-P. Li, O.-Y. Jing-Ping, J.-F. Stoltz, A. Eljaafari, Evaluation of Human MSCs Cell Cycle, Viability and Differentiation in Micromass Culture, IOS Press, 2006.
[12] H.J. Jin, S.K. Park, W. Oh, Y.S. Yang, S.W. Kim, S.J. Choi, Down-regulation of CD105 is associated with multi-lineage differentiation in human umbilical cord blood-derived mesenchymal stem cells, Biochem. Biophys. Res. Commun. 381 (2009) 676–681, https://doi.org/10.1016/j.bbrc.2009.02.118.
[13] B. Delorme, J. Ringe, N. Gallay, Y. le Vern, D. Kerboeuf, C. Jorgensen, P. Rosset, L. Sensebé, P. Layrolle, T. Hä, P. Charbord, Specific plasma membrane protein phenotype of culture-amplified and native human bone marrow mesenchymal stem cells. https://doi.org/10.1182/blood-2007-07, 2008.
[14] C. Vater, P. Kasten, M. Stiehler, Culture media for the differentiation of mesenchymal stromal cells, Acta Biomater. 7 (2011) 463–477, https://doi.org/10.1016/j.actbio.2010.07.037.
[15] M.J. Dalby, N. Gadegaard, R.O.C. Oreffo, Harnessing nanotopography and integrin-matrix interactions to influence stem cell fate, Nat. Mater. 13 (2014) 558–569, https://doi.org/10.1038/nmat3980.
[16] R.J. McMurray, N. Gadegaard, P.M. Tsimbouri, K.v. Burgess, L.E. McNamara, R. Tare, K. Murawski, E. Kingham, R.O.C. Oreffo, M.J. Dalby, Nanoscale surfaces for the long-term maintenance of mesenchymal stem cell phenotype and multipotency, Nat. Mater. 10 (2011) 637–644, https://doi.org/10.1038/nmat3058.
[17] D.C.L. Rowland, T. Aquilina, A. Klein, O. Hakimi, P. Alexis-Mouthuy, A.J. Carr, S.J.B. Snelling, A comparative evaluation of the effect of polymer chemistry and fiber orientation on mesenchymal stem cell differentiation, J. Biomed. Mater. Res. 104 (2016) 2843–2853, https://doi.org/10.1002/jbm.a.35829.
[18] S. Nedjari, F. Awaja, R. Guarino, D. Gugutkov, G. Altankov, Establishing multiple osteogenic differentiation pathways of mesenchymal stem cells through different scaffold configurations, J Tissue Eng Regen Med 14 (2020) 1428–1437, https://doi.org/10.1002/term.3108.
[19] P.Y. Wang, L.R. Clements, H. Thissen, A. Jane, W.B. Tsai, N.H. Voelcker, Screening mesenchymal stem cell attachment and differentiation on porous silicon gradients, Adv. Funct. Mater. 22 (2012) 3414–3423, https://doi.org/10.1002/adfm.201200447.
[20] A.J. Engler, S. Sen, H.L. Sweeney, D.E. Discher, Matrix elasticity directs stem cell lineage specification, Cell 126 (2006) 677–689, https://doi.org/10.1016/j.cell.2006.06.044.
[21] M. Guillot-Ferriols, S. Lanceros-Méndez, J.L. Gómez Ribelles, G. Gallego Ferrer, Electrical stimulation: effective cue to direct osteogenic differentiation of mesenchymal stem cells? Biomater. Adv. 138 (2022) 212918 https://doi.org/10.1016/j.bioadv.2022.212918.

[22] A. Halim, A.D. Ariyanti, Q. Luo, G. Song, Recent progress in engineering mesenchymal stem cell differentiation, Stem Cell Rev Rep 16 (2020) 661–674, https://doi.org/10.1007/s12015-020-09979-4.

[23] J. Parssinen, H. Hammarén, R. Rahikainen, V. Sencadas, C. Ribeiro, S. Vanhatupa, S. Miettinen, S. Lanceros-Méndez, V.P. Hytönen, Enhancement of adhesion and promotion of osteogenic differentiation of human adipose stem cells by poled electroactive poly(vinylidene fluoride), J. Biomed. Mater. Res. 103 (2015) 919–928, https://doi.org/10.1002/jbm.a.35234.

[24] J. Li, X. Mou, J. Qiu, S. Wang, D. Wang, D. Sun, W. Guo, D. Li, A. Kumar, X. Yang, A. Li, H. Liu, Surface charge regulation of osteogenic differentiation of mesenchymal stem cell on polarized ferroelectric crystal substrate, Adv. Healthcare Mater. 4 (2015) 998–1003, https://doi.org/10.1002/adhm.201500032.

[25] Z. Zhou, W. Li, T. He, L. Qian, G. Tan, C. Ning, Polarization of an electroactive functional film on titanium for inducing osteogenic differentiation, Sci. Rep. 6 (2016), https://doi.org/10.1038/srep35512.

[26] A. Samadi, M.A. Salati, A. Safari, M. Jouyandeh, M. Barani, N.P. Singh Chauhan, E.G. Golab, P. Zarrintaj, S. Kar, F. Seidi, A. Hejna, M.R. Saeb, Comparative review of piezoelectric biomaterials approach for bone tissue engineering, J. Biomater. Sci. Polym. Ed. 33 (2022) 1555–1594, https://doi.org/10.1080/09205063.2022.2065409.

[27] M. Guillot-Ferriols, J.C. Rodríguez-Hernández, D.M. Correia, S.A.C. Carabineiro, S. Lanceros-Méndez, J.L. Gómez Ribelles, G. Gallego Ferrer, Poly(vinylidene) fluoride membranes coated by heparin/collagen layer-by-layer, smart biomimetic approaches for mesenchymal stem cell culture, Mater. Sci. Eng. C 117 (2020), https://doi.org/10.1016/j.msec.2020.111281.

[28] X. Sun, Y. Bai, X. Zheng, X. Li, Y. Zhou, Y. Wang, B.C. Heng, X. Zhang, Bone piezoelectricity-mimicking nanocomposite membranes enhance osteogenic differentiation of bone marrow mesenchymal stem cells by amplifying cell adhesion and actin cytoskeleton, J. Biomed. Nanotechnol. 17 (2021) 1058–1067, https://doi.org/10.1166/jbn.2021.3090.

[29] M.F. Abazari, F. Soleimanifar, M. Amini Faskhodi, R.N. Mansour, J. Amini Mahabadi, S. Sadeghi, H. Hassannia, E. Saburi, S.E. Enderami, M.M. Khani, S. Zare Karizi, Improved osteogenic differentiation of human induced pluripotent stem cells cultured on polyvinylidene fluoride/collagen/platelet-rich plasma composite nanofibers, J. Cell. Physiol. 235 (2020) 1155–1164, https://doi.org/10.1002/jcp.29029.

[30] M.F. Abazari, F. Soleimanifar, S.E. Enderami, M. Nematzadeh, N. Nasiri, F. Nejati, E. Saburi, S. Khodashenas, B. Darbasizadeh, M.M. Khani, P. Ghoraeian, Incorporated-bFGF polycaprolactone/polyvinylidene fluoride nanocomposite scaffold promotes human induced pluripotent stem cells osteogenic differentiation, J. Cell. Biochem. 120 (2019) 16750–16759, https://doi.org/10.1002/jcb.28933.

[31] V. Sencadas, R. Gregorio, S. Lanceros-Méndez, α to β phase transformation and microestructural changes of PVDF films induced by uniaxial stretch, J. Macromol. Sci., Part B: Phys. 48 (2009) 514–525, https://doi.org/10.1080/00222340902837527.

[32] P. Martins, A.C. Lopes, S. Lanceros-Mendez, Electroactive phases of poly(vinylidene fluoride): determination, processing and applications, Prog. Polym. Sci. 39 (2014) 683–706, https://doi.org/10.1016/j.progpolymsci.2013.07.006.

[33] C. Ribeiro, J.A. Panadero, V. Sencadas, S. Lanceros-Méndez, M.N. Tamaño, D. Moratal, M. Salmerón-Sánchez, J.L. Gómez Ribelles, Fibronectin adsorption and cell response on electroactive poly(vinylidene fluoride) films, Biomed. Mater. 7 (2012), https://doi.org/10.1088/1748-6041/7/3/035004.

[34] J. Parssinen, H. Hammarén, R. Rahikainen, V. Sencadas, C. Ribeiro, S. Vanhatupa, S. Miettinen, S. Lanceros-Méndez, V.P. Hytönen, Enhancement of adhesion and promotion of osteogenic differentiation of human adipose stem cells by poled electroactive poly(vinylidene fluoride), J. Biomed. Mater. Res. 103 (2015) 919–928, https://doi.org/10.1002/jbm.a.35234.

[35] R. Sobreiro-Almeida, M.N. Tamaño-Machiavello, E.O. Carvalho, L. Cordón, S. Doria, L. Senent, D.M. Correia, C. Ribeiro, S. Lanceros-Méndez, R. Sabater I Serra, J.L. Gomez Ribelles, A. Sempere, Human mesenchymal stem cells growth and osteogenic differentiation on piezoelectric poly(Vinylidene fluoride) microsphere substrates, Int. J. Mol. Sci. 18 (2017), https://doi.org/10.3390/ijms18112391.

[36] M.P. Silva, C.M. Costa, V. Sencadas, A.J. Paleo, S. Lanceros-Méndez, Degradation of the dielectric and piezoelectric response of β-poly(vinylidene fluoride) after temperature annealing, J. Polym. Res. 18 (2011) 1451–1457, https://doi.org/10.1007/s10965-010-9550-x.

[37] V. Sencadas, C.M. Costa, V. Moreira, J. Monteiro, S.K. Mendiratta, J.F. Mano, S. Lanceros-Méndez, Poling of β-poly(vinylidene fluoride): dielectric and IR spectroscopy studies. http://www.e-polymers.org, 2005.

[38] M.F. Pittenger, A.M. Mackay, S.C. Beck, R.K. Jaiswal, R. Douglas, J.D. Mosca, M.A. Moorman, D.W. Simonetti, S. Craig, D.R. Marshak, Multilineage potential of adult human mesenchymal stem cells, Science 284 (1999) (1979) 143–147, https://doi.org/10.1126/science.284.5411.143.

[39] C. Ribeiro, C.M. Costa, D.M. Correia, J. Nunes-Pereira, J. Oliveira, P. Martins, R. Gonçalves, V.F. Cardoso, S. Lanceros-Méndez, Electroactive poly(vinylidene fluoride)-based structures for advanced applications, Nat. Protoc. 13 (2018) 681–704, https://doi.org/10.1038/nprot.2017.157.

[40] E.O. Carvalho, M.M. Fernandes, J. Padrao, A. Nicolau, J. Marqués-Marchán, A. Asenjo, F.M. Gama, C. Ribeiro, S. Lanceros-Mendez, Tailoring bacteria response by piezoelectric stimulation, ACS Appl. Mater. Interfaces 11 (2019) 27297–27305, https://doi.org/10.1021/acsami.9b05013.

[41] P.M. Martins, S. Ribeiro, C. Ribeiro, V. Sencadas, A.C. Gomes, F.M. Gama, S. Lanceros-Méndez, Effect of poling state and morphology of piezoelectric poly (vinylidene fluoride) membranes for skeletal muscle tissue engineering, RSC Adv. 3 (2013) 17938–17944, https://doi.org/10.1039/c3ra43499k.

[42] J. Parssinen, H. Hammarén, R. Rahikainen, V. Sencadas, C. Ribeiro, S. Vanhatupa, S. Miettinen, S. Lanceros-Méndez, V.P. Hytönen, Enhancement of adhesion and promotion of osteogenic differentiation of human adipose stem cells by poled electroactive poly(vinylidene fluoride), J. Biomed. Mater. Res. 103 (2015) 919–928, https://doi.org/10.1002/jbm.a.35234.

[43] H.J. Jin, S.K. Park, W. Oh, Y.S. Yang, S.W. Kim, S.J. Choi, Down-regulation of CD105 is associated with multi-lineage differentiation in human umbilical cord blood-derived mesenchymal stem cells, Biochem. Biophys. Res. Commun. 381 (2009) 676–681, https://doi.org/10.1016/j.bbrc.2009.02.118.

[44] J.-W. Yang, N. de Isla, C. Huselstein, M.-N. Sarda-Kolopp, N. Li, Y.-P. Li, O.-Y. Jing-Ping, J.-F. Stoltz, A. Eljaafari, Evaluation of Human MSCs Cell Cycle, Viability and Differentiation in Micromass Culture, IOS Press, 2006.

[45] P. Ducy, R. Zhang, Osf2/Cbfa1: A Transcriptional Activator of Osteoblast Differentiation, 1997.

[46] B. Kern, J. Shen, M. Starbuck, G. Karsenty, Cbfa1 contributes to the osteoblast-specific expression of type I collagen genes, J. Biol. Chem. 276 (2001) 7101–7107, https://doi.org/10.1074/jbc.M006215200.

[47] D. Pavlin, J. Gluhak-Heinrich, Effect of mechanical loading on periodontal cells, Crit. Rev. Oral Biol. Med. 12 (2001) 414–424, https://doi.org/10.1177/10454411010120050401.

[48] D. Pavlin, R. Zadro, J. Gluhak-Heinrichb, Temporal Pattern of Stimulation of Osteoblast-Associated Genes during Mechanically-Induced Osteogenesis in Vivo: Early Responses of Osteocalcin and Type I Collagen, n.D. .

[49] V. Ronique Lefebvre, W. Huang, V.R. Harley, P.N. Goodfellow, B. de Crombrugghe, SOX9 is a potent activator of the chondrocyte-specific enhancer of the Pro1 (II), Collagen Gene (1997). http://mcb.asm.org/.

[50] H. Lu, L. Guo, M.J. Wozniak, N. Kawazoe, T. Tateishi, X. Zhang, G. Chen, Effect of cell density on adipogenic differentiation of mesenchymal stem cells, Biochem. Biophys. Res. Commun. 381 (2009) 322–327, https://doi.org/10.1016/j.bbrc.2009.01.174.

[51] S. Trivedi, K. Srivastava, A. Gupta, T.S. Saluja, S. Kumar, D. Mehrotra, S.K. Singh, A quantitative method to determine osteogenic differentiation aptness of scaffold, J Oral Biol Craniofac Res 10 (2020) 158–160, https://doi.org/10.1016/j.jobcr.2020.04.006.

[52] L. Mao, L. Bai, X. Wang, X. Chen, D. Zhang, F. Chen, C. Liu, Enhanced cell osteogenesis and osteoimmunology regulated by piezoelectric biomaterials with controllable surface potential and charges, ACS Appl. Mater. Interfaces 14 (2022) 44111–44124, https://doi.org/10.1021/acsami.2c11131.

[53] B. Ganss, R.H. Kim, J. Sodek, Bone sialoprotein, Crit. Rev. Oral Biol. Med. 10 (1999) 79–98, https://doi.org/10.1177/10454411990100010401.

[54] A. Oldberg, A. Franzen, D. Heinegard, The primary structure of a cell-binding bone sialoprotein, J. Biol. Chem. 263 (1988) 19430–19432, https://doi.org/10.1016/s0021-9258(19)77651-0.

[55] Z. Zhou, W. Li, T. He, L. Qian, G. Tan, C. Ning, Polarization of an electroactive functional film on titanium for inducing osteogenic differentiation, Sci. Rep. 6 (2016), https://doi.org/10.1038/srep35512.

[56] R. Mcbeath, D.M. Pirone, C.M. Nelson, K. Bhadriraju, C.S. Chen, Cell Shape, Cytoskeletal Tension, RhoA regulate stem cell lineage commitment, Dev. Cell 6 (2004) 483–495. http://www.developmentalcell.com/cgi/.

[57] K.A. Kilian, B. Bugarija, B.T. Lahn, M. Mrksich, Geometric cues for directing the differentiation of mesenchymal stem cells, Proc. Natl. Acad. Sci. U. S. A. 107 (2010) 4872–4877, https://doi.org/10.1073/pnas.0903269107.

[58] J. Parssinen, H. Hammarén, R. Rahikainen, V. Sencadas, C. Ribeiro, S. Vanhatupa, S. Miettinen, S. Lanceros-Méndez, V.P. Hytönen, Enhancement of adhesion and promotion of osteogenic differentiation of human adipose stem cells by poled electroactive poly(vinylidene fluoride), J. Biomed. Mater. Res. 103 (2015) 919–928, https://doi.org/10.1002/jbm.a.35234.
[59] B. Geng, F. Fang, P. Li, S. Xu, D. Pan, Y. Zhang, L. Shen, Surface charge-dependent osteogenic behaviors of edge-functionalized graphene quantum dots, Chem. Eng. J. 417 (2021), https://doi.org/10.1016/j.cej.2020.128125.
[60] A.E. Eldeeb, S. Salah, N.A. Elkasabgy, Biomaterials for tissue engineering applications and current updates in the field: a comprehensive review, AAPS PharmSciTech 23 (2022), https://doi.org/10.1208/s12249-022-02419-1.